Strategy to shape, on a half-meter scale, a geopolymer composite structure by additive manufacturing

Julien Archez, Sébastien Maitenaz, Leo Demont, M. Charrier, Romain Mesnil, Nathalie Texier-Mandoki, Xavier Bourbon, Sylvie Rossignol, Jean-François Caron

Strategy to shape, on a half-meter scale, a geopolymer composite structure by additive manufacturing

J. Archez[1,2,3], S. Maitenaz[3], L. Demont[3], M. Charrier[3], R. Mesnil[3], N. Texier-Mandoki[2], X. Bourbon[2], S. Rossignol[1*] and J.F. Caron[3].

[1] IRCER: Institut de Recherche sur les Céramiques (UMR7315), 12 rue Atlantis, 87068 Limoges Cedex, France.

[2] Agence nationale pour la gestion des déchets radioactifs (Andra), 1/7 rue Jean-Monnet 92298 Chatenay-Malabry, France.

[3] Laboratoire Navier, UMR 8205, Ecole des Ponts, CNRS, UPE, Champs-sur-Marne, France

*Corresponding author: sylvie.rossignol@unilim.fr, tel.: 33 5 87 50 25 64

Abstract

This work aims at proposing a strategy for 3D-printing geopolymer composite structures at a half-meter scale, without using organic additives. An original printing device based on cartridges is developed and adapted to a 6-axis robot. The yield stress, working time and apparent Young modulus of the extruded material are measured. A devoted software, procedure and printing path are set up, leading to the fabrication of a structure without height limitation, without major geometrical defects or instabilities. The working time ensures the consolidation of the material during printing and good adhesion between layers. As an example, four successive cartridges have been successfully used to elaborate a hollow cylinder (Φ = 35 cm, H = 45 cm).

Keywords: Geopolymer, Composite, Additive manufacturing, Structure, Robot, Large scale.

1. INTRODUCTION

This study is part of the Cigéo project led by the French National Radioactive Waste Management Agency (Andra) for long-term management of the high and intermediate-level radioactive waste in deep-geological medium. Andra is looking for alternatives materials to metallic tunnel liners. These liners (rigid tubes Φ = 70 cm, L = 100 cm) bear the geological mechanical stresses. 3D printed geopolymer composites without organic additives are investigated here and different suitable formulations were previously proposed in [1, 2], including wollastonite and glass fibers. Strengths are found similar to cast samples [3]. Printing of geopolymers has already been done at a small scale (mm) using organic additives [4] and at a larger scale (cm), with alkali-activated materials [5, 6] and organic additives (microalgae) [7]. At larger scales, many structures were extruded from cementitious materials [8]. However, the hardening process of geopolymer is different from cement pastes, and the shaping process had to be adapted.

This article aims at proposing a printing strategy for large structures, without the use of organic additives. A cartridge-based 3D-printer adapted to an industrial robot is first developed. Rheological parameters are then identified to address the material settlement and to print a structure without height limitation.

2. MATERIALS AND METHODS

For technical, reproducibility, and safety reasons, an extrusion tool based on four-liter cartridges is developed and mounted on a 6 axis robot *ABB-IRB-6620* (**Figure 1-a**). The process is controlled with *HAL Robotics* software, and a pneumatic extruder pushes the material through a 15 mm nozzle. A worm screw regulates the flow rate (**Figure 1-b**). Several cartridges are successively used.

The settlement is caused by an initial crushing due to extrusion, followed by a progressive deformation of the layers (Δh). As Δh increases linearly with weight of successive layers, it can be described as an apparent elastic deformation (**Equation 1**) due to the elastic part of this Herschel-Bulkley material until yield stress (it probably exists also a strain hardening deformation contribution as the material is elasto-plastic). The experimental value of the apparent Young modulus is identified on a first printing. It enables to estimate the settlement of the material and to adapt the robot path for the next print in order to keep a constant nozzle-lace distance during printing, avoiding gaps and collapses as in **Figure 3-a,b**.

$$\Delta h = \int_0^h \varepsilon(z)\, dz = \int_0^h \frac{\sigma(\mathrm{z})}{\mathrm{E}}\,\mathrm{dz} = \int_0^{\mathrm{h}} \frac{\rho \mathrm{g}(\mathrm{h}-\mathrm{z})}{\mathrm{E}}\,\mathrm{dz} = \frac{\rho \mathrm{g h}^2}{2\mathrm{E}} \qquad \textbf{(1)}$$

With $\varepsilon(z)$ the elastic strain, h (m) the structure height, and E (Pa) the apparent Young modulus of the fresh material.

Based on previous studies [1, 2], a formulation composed with metakaolin (M1000 from Imerys), potassium alkaline solution (Woellner), wollastonite (Imerys), and glass fibers (L= 6 mm, Owens Corning) is chosen. The extrusion started 35 minutes after the mixing start and the printed material was cured at 20 °C.

It has been shown that the yield stress of the printed material permits to determine a critical printing height (**Equation 2**) [9]. If this critical height is exceeded, the Herschel-Buckley type material starts to flow and the structure collapses. As demonstrated in [10] for visco-plastic materials and more recently for cementitious materials [11], the yield stress is analytically linked to the mass of a drop and the radius of the nozzle outlet.

$$H_{critical} = \frac{\sqrt{3}\tau_0}{\rho g} \quad \textbf{(2)}$$

With $H_{critical}$ (m) the critical printing height, τ_0 (Pa) the yield stress, ρ (kg/m^3) the density, and g (m²/s) the gravity acceleration.

The working time is assessed with a standardized Vicat measurement [12]. The 300 g needle is released on the geopolymer lace surface and its penetration depth is measured.

3. RESULTS

Yield stress has been measured over time for two different worm screw speeds (0.16 and 1.60 rotations/s) corresponding to measured flow rates of 0.9 and 8.5 g/s respectively (**Figure 2-a**). Regardless of the worm screw speed, the yield stress increased from 1900 to 2900 Pa during the first 8 minutes of extrusion due to the polycondensation reactions. With the lowest flow rate, the yield stress continued to increase until blocking the extrusion when reaching 4395 Pa at 40 min. The increase of yield stress allows to stack up more layers but also decreases the pumpability and the quality of the layers interfaces [7]. High worm screw speed and flow rate are then recommended. The Vicat needle penetration depth (**Figure 2-b**) has been measured over time for three laces having different initial yield stress (2282 Pa, 3046 Pa, and 3542 Pa) since collected at three different extrusion times (4, 13, and 30 min). The needle penetration depth decreases as the yield stress increases. At 80 minutes, all the curve converges and the material can be considered as consolidated (t_{Vicat}) while still fresh. This permits to estimate the time-dependent capacity of a lace to support and bond the upper layers. A precise timing can be set with adaptable parameters such as the formulation (yield stress, working time), process (nozzle dimension, flow rate, printing speed), and structure (dimensions, printing path, layers height). For instance, when stacking an identical layer path, **Equation 3** gives the time between batches to continue the printing without reaching the critical printing height.

$$t = \frac{H_{critical} \times P}{v_n \times h_l} - t_{Vicat} \quad \textbf{(3)}$$

With t (s) the time between batches, t_{Vicat} (s) the working time, v_n (m/s) the nozzle speed, h_l (m) the layer height, and P (m) the printing path of one layer.

All these identifications must be integrated into a simulation, to define optimized parameters to print a given structure.

A first print was made without correction of the printing path (**Figure 3-a**), and excessive settlement of the material is observed. This settlement increases continuously, leading to a gap between the nozzle and the last layer. With such a high gap, the layers are not stacked

precisely and the printing had to be stopped during the first cartridge step. The gap can be estimated using **Equation 1** and the robot path corrected. Twenty-five layers (33 cm) have then been stacked correctly without any gap **(Figure 3-b)**. However, with a yield stress of 2100 Pa, the critical height (18.5 cm deduced from **Equation 2**) has been exceeded resulting in local geometric imperfections and structural instabilities. The structure collapsed at the 26^{th} layer. Compared with the previous test, the timing between the successive cartridges was precisely estimated and the control of the hardening evolution was achieved (**Figure 3-c**). It permits both a sufficient resistance to settlement and a good adhesion between layers as shown in a cross-section of a printing sample in **Figure 3-d**. Finally, a hollow cylinder (Φ = 34 cm, H = 45 cm, thickness = 1.5 cm) elaborated with four cartridges and a time between cartridges of 70 minutes shows regular layer stacking and presents almost no defects, even if the settlement of the material lead to a 1 cm difference between the diameters at the bottom (35 cm) and at the top (34 cm) of the cylinder. The use of a material with higher yield stress could drastically reduce this value. By increasing the number of cartridges, the structure dimensions could be increased without issue (within the process limits). The elaboration of this structure validates the strategy carried out and is a half-scale demonstrator of how a geopolymer composite liner could be shaped.

4. CONCLUSION

This study focuses on the shaping of geopolymer composites formulated without any organic additives, at a meter scale, with an additive manufacturing process. A cartridge-based extruder is developed and mounted on a 6-axis robot. The consistency of the material at the outlet of the nozzle, the working time, and the settlement of the stacking sequence, were assessed. The key characteristics (yield stress, working time) were then identified to determine a time between cartridges in relation to the process parameters (nozzle size and speed, layer height) and a printing path correction method. Finally, a half-scale demonstrator of a geopolymer liner for high-level radioactive waste cell was successfully printed. Upscaling is thus conceivable with the use of geopolymer composite material and the developed strategy. Some aspects of the process should be improved for industrial applications. The cartridge supply may be automated, but the most promising direction seems to develop a more sophisticated continuous or semi-continuous printing system, like those seen in large-scale 3D concrete printing.

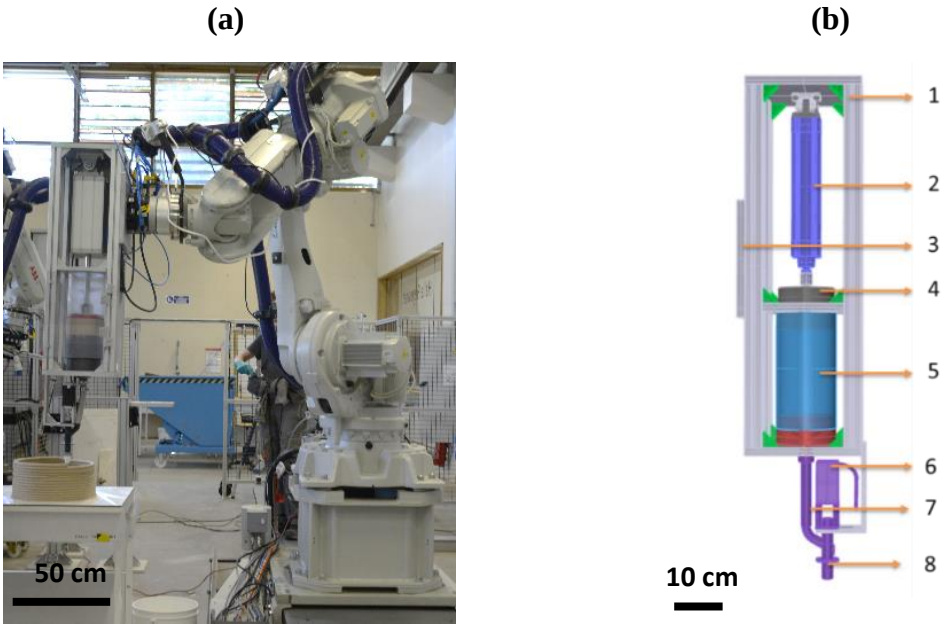

Figure 1. (a) printing system and **(b)** cartridge extruder: (1) frame, (2) pneumatic cylinder (3) tool changer (4), piston, (5) cartridge, (6) stepper motor, (7) pipe and (8) worm screw.

(a)

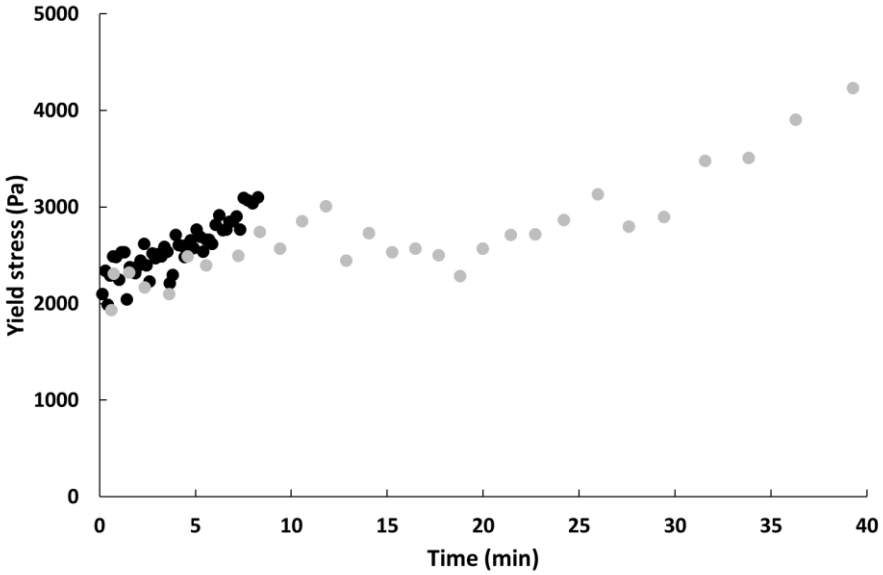

(b)

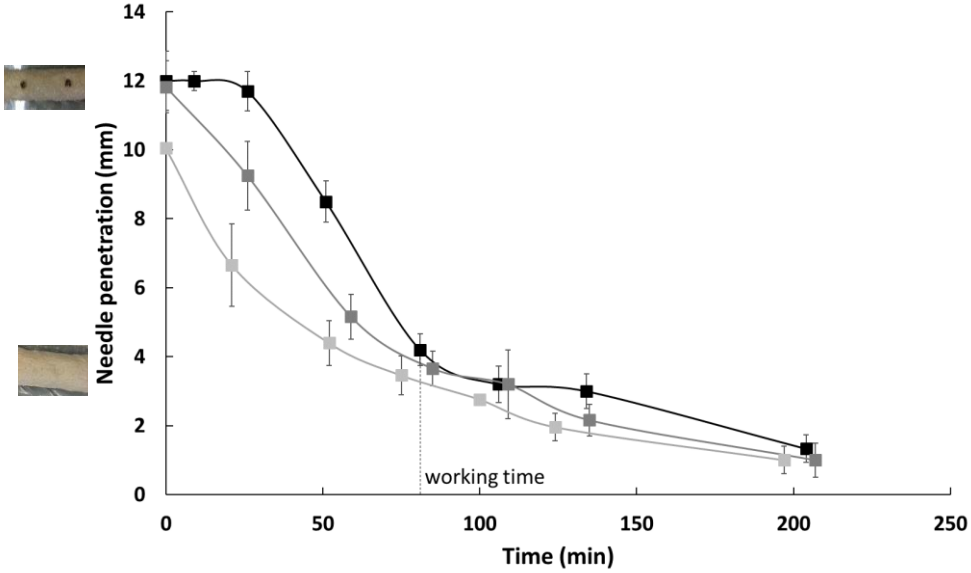

Figure 2. (a) Yield stress evolution for a worm screw speed of ● 0.16 and ● 1.60 rotations/s and **(b)** needle penetration evolution for three different extrusion time corresponding with three yield stress (■ 4 min / 2282 Pa, ■ 13 min / 3046 Pa and ■ 30 min / 3542 Pa).

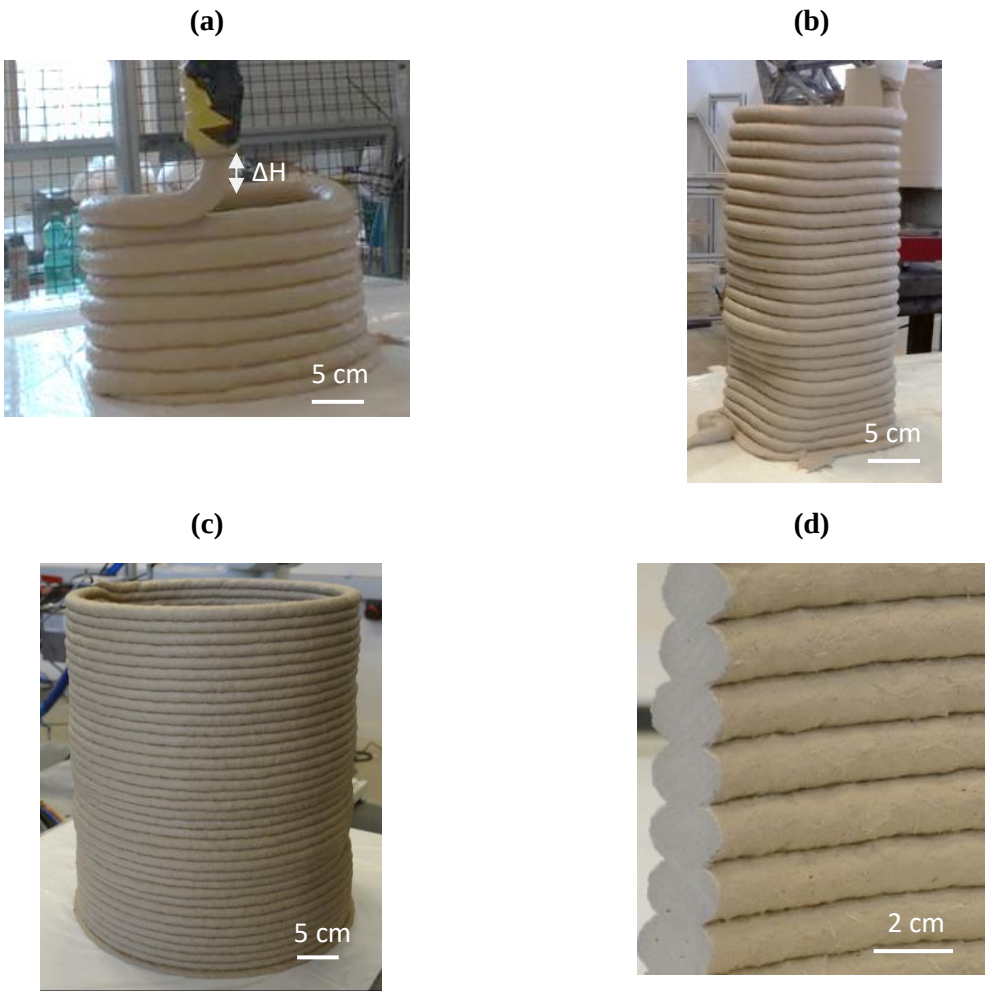

Figure 3. Photos of **(a)** an important gap (ΔH), **(b)** an exceedance of the critical height and a resulting collapse, **(c)** a mastered printing with four cartridges and larger dimensions (Φ = 35 cm, H = 45 cm) and **(d)** a cross-section of a printed sample.

5. REFERENCES

[1] J. Archez et al. 2020. Influence of the aluminum concentration, wollastonite and glass fibers on geopolymer composites workability and mechanical properties. Construction and Building Materials. 119511. 10.1016/j.conbuildmat.2020.119511.
[2] J. Archez et al., 2020. Adaptation of the geopolymer composite formulation to the shaping process. Journal of Building Engineering, 101501. 10.1016/j.mtcomm.2020.101501.
[3] J. Archez et al., 2020. Shaping of geopolymer composites by 3D printing. Materials Today Communication, 25, 101894. https://doi.org/10.1016/j.jobe.2020.101894.
[4] G. Franchin et al., 2017. Direct ink writing of geopolymeric inks. Journal of the European Ceramic Society. 37, 2481-2489. 10.1016/j.jeurceramsoc.2017.01.030.
[5] B. Panda et al. 2019. Extrusion and rheology characterization of geopolymer nanocomposites used in 3D printing. Composites part B. 176, 107290. 10.1016/j.compositesb.2019.107290.
[6] D.-W. Zhang et al. 2018. The study of the structure rebuilding and yield stress of 3D printing geopolymer pastes. Construction and Building Materials. 184, 575-580. 10.1016/j.conbuildmat.2018.06.233
[7] E. Agnoli et al. 2019. Additive Manufacturing of Geopolymers Modified with Microalgal Biomass Biofiller from Wastewater Treatment Plants. Materials. 12, 1004. 10.3390/ma12071004.

[8] C. Gosselin et al. 2016. Large-scale 3D printing of ultra-high performance concrete. Materials and design. 100, 102-109. 10.1016/j.matdes.2016.03.097.
[9] N. Roussel, 2018. Rheological requirements for printable concretes. Cement and Concrete Research. 112, 76-85. 10.1016/j.cemconres.2018.04.005.
[10] P. Coussot et al. 2005. Gravity flow instability of viscoplastic materials: The ketchup drip, *Phys. Rev. E*, 72, 031409, 2005. 10.1103/PhysRevE.72.031409.
[11] N. Ducoulombier et al. 2020. The Slug test: Inline assessment of Yield Stress for Extrusion-based Additive Manufacturing. Digital Concrete. 216-224. 10.1007/978-3-030-49916-7_22.
[12] French standard, NF EN 480-2, 2006.